

High-resolution polarization analysis study of long-range magnetic order in cuprates

Zahirul Islam,* D. Haskel, J. C. Lang, and G. Srajer

Advanced Photon Source, Argonne National Laboratory, 9700 South Cass Avenue, Argonne, Illinois 60439, USA

X. Liu and S. K. Sinha

Physics Department, University of San Diego, La Jolla, California 92093, USA

B. W. Veal

Materials Science Division, Argonne National Laboratory, 9700 South Cass Avenue, Argonne, Illinois 60439, USA

(Received 6 December 2004; published 28 June 2005)

We demonstrate how x-ray nonresonant magnetic scattering can be successfully used to study long-range-ordered spin- $\frac{1}{2}$ moments in cuprates. We studied the antiferromagnetic state characterized by $\mathbf{q}_{\text{AF}} = (\frac{1}{2}, \frac{1}{2}, 0)$, in high-quality single crystals of yttrium barium copper oxides, $\text{YBa}_2\text{Cu}_3\text{O}_{6+x}$ ($x \sim 0.14$ and ~ 0.20). We found magnetic correlation lengths of at least $\sim 1000 \text{ \AA}$ in all directions. The polarization analysis and momentum dependence of magnetic Bragg peaks are consistent with the magnetic scattering cross section. No detectable magnetic scattering corresponding to $(\frac{1}{2}, \frac{1}{2}, \frac{1}{2})$ was observed.

DOI: 10.1103/PhysRevB.71.212506

PACS number(s): 74.72.Bk, 75.25.+z, 75.30.-m, 61.10.Eq

The antiferromagnetic (AF) ground state in the parent compound of cuprate-based superconductors, such as lanthanum copper oxides ($\text{La}_2\text{CuO}_{4+\delta}$), has been well characterized by neutron-scattering measurements.¹⁻³ These measurements found magnetic ordering characterized by the wave vector $\mathbf{q}_{\text{AF}} = (\frac{1}{2}, \frac{1}{2}, 0)$, which disappears above a temperature where a peak in the magnetic susceptibility in these compounds is observed. In the case of yttrium barium copper oxides ($\text{YBa}_2\text{Cu}_3\text{O}_{6+x}$, YBCO), however, susceptibility measurements on insulating compounds with low oxygen concentrations showed no obvious signs of any phase transition into a magnetically ordered state. Although early muon spin relaxation (μSR) measurements⁴ indicated a magnetically long-range-ordered state in YBCO with low oxygen concentrations, it was not until neutron diffraction studies⁵⁻¹⁰ were carried out that the magnetic structure of these materials was revealed. These studies showed that the AF state in YBCO is also characterized by the wave vector \mathbf{q}_{AF} . This magnetic structure corresponds to a doubling of the chemical unit cell within the square CuO_2 layers (ab planes), with the ordered copper moments aligned in these planes. However, some of these studies^{10,11} observed a second magnetic transition in YBCO with an O concentration of $x \sim 0.35$, at a temperature well below the Néel temperature, characterized by a wave vector $(\frac{1}{2}, \frac{1}{2}, \frac{1}{2})$, indicating an additional doubling of the unit cell along the tetragonal c -axis. This low-temperature phase is due to the ordering of moments in the O-deficient CuO chains located in between next-nearest-neighbor CuO_2 planes. Although the understanding of this low-temperature ordered phase is very poor in the context of the electronic phase diagram, such a magnetic state is unlikely to occur at low O concentration as the number of moment-bearing Cu^{2+} ions in the O-deficient chains decreases with compositions approaching that of the stoichiometric $\text{YBa}_2\text{Cu}_3\text{O}_6$. Furthermore, this magnetic phase was found to be very sensitive to the O stoichiometry, chemical and structural homogeneity of the samples.¹¹

A technique, such as magnetic scattering of x rays,¹²⁻¹⁴ is well suited for studying such phenomena in small but high-quality single-crystal samples. At third-generation synchrotron facilities, a focused undulator beam has sufficient brilliance for measurements on samples with submillimeter dimensions. Since sample homogeneity and quality are, in general, superior in small crystals, one may eliminate spurious effects associated with sample inhomogeneity. To date, however, x-ray magnetic scattering studies of copper moments in pure YBCO compounds have not been successful because of the weakness of scattering cross section relative to Thomson scattering, insufficient suppression of background, and poor sample quality. In this work, we have succeeded in observing the magnetic ground state of 3D-ordered copper moments in two well-prepared crystals of YBCO with nominal compositions of $x \sim 0.20$ and $x \sim 0.14$, respectively, using nonresonant magnetic scattering of x rays. A long-range-ordered (correlation length, $\xi \sim 1000 \text{ \AA}$) AF state characterized by \mathbf{q}_{AF} was clearly observed in both cases. Polarization analysis and momentum dependence of the magnetic Bragg peaks are consistent with a nonresonant scattering cross section of x rays. We looked for the low- T magnetic structure characterized by $(\frac{1}{2}, \frac{1}{2}, \frac{1}{2})$ in the sample with $x \sim 0.20$ and did not find any evidence within our detectability limits at $\sim 10 \text{ K}$. Although it is not conclusive, based on an earlier study¹⁰ and our observation, we can speculate that at this temperature either an ordered cell-doubling magnetic phase is not stable for O concentrations less than some cutoff that must be greater than $x=0.20$, or the magnitude of the ordered copper moments in the chains is substantially smaller than $0.5-0.6 \mu_B$ per copper in the CuO_2 planes.^{5,6}

Magnetic scattering studies were carried out on the 4ID-D beamline of the Advanced Photon Source. A monochromatic beam from a double-bounce $\text{Si}(111)$ crystal monochromator was focused vertically and horizontally by a Pd mirror to a spot size of $150 \mu\text{m} \times 200 \mu\text{m}$, delivering $\sim 10^{13}$ photons/s at the sample. Since the magnetic scattering is extremely

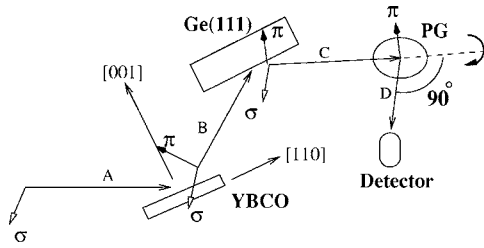


FIG. 1. High-resolution polarization analysis setup. (A) σ -polarized (empty arrow) incoming x-ray beam; (B) magnetically scattered beam with both σ and π (filled arrow) components; (C) diffracted beam from the Ge(111) analyzer; (D) polarization analyzed beam by PG; in the $\sigma\pi$ channel the PG is rotated about the dashed line in order to diffract perpendicular to the vertical scattering plane. (A), (B), and (C), all lie in the vertical scattering plane.

weak and detecting nonresonant scattering from ordered spin- $\frac{1}{2}$ moments is a formidable task, we focused on eliminating the charge-scattering contribution as much as possible. First, we used a Ge(1 1 1) analyzer crystal to improve resolution and reduce background. Then a pyrolytic graphite (PG) crystal was placed after the Ge analyzer so that the PG(006) reflection could be used as an x-ray polarization analyzer.¹⁵ This setup kept the background count rate to a very low ~ 0.2 counts/s. The synchrotron x rays from the undulator are linearly polarized in the orbital plane (horizontal) of the storage-ring electrons. With respect to the vertical scattering plane employed in this work, this state of polarization is designated as σ . Unlike Thomson scattering, magnetically scattered photons develop a component of polarization in the vertical scattering plane (π polarization). In order to get the maximum suppression of charge scattering, we chose the incident energy to be 7.848 keV [$\theta_B \approx 45^\circ$ for the PG(0 0 6) reflection] at which point the contributions from

σ -polarized scattered photons can be efficiently suppressed by setting the PG crystal to diffract at 90° with respect to the vertical scattering plane ($\sigma\pi$ channel). When the PG crystal diffracts within the vertical plane unrotated σ -polarized photons are detected ($\sigma\sigma$ channel). Figure 1 gives a schematic of the polarization analysis setup. We note that magnetic scattering was also observed without the use of the Ge analyzer since the key element was the exact polarization analyzer. However, the resolution and the peak-to-background ratio were not as good.

The single crystals studied were grown by the self-flux¹⁶ method. They were $\sim 70\text{-}\mu\text{m}$ -thick rectangular plates with dimensions of $2\text{ mm} \times 3\text{ mm}$ ($x \sim 0.14$) and $1\text{ mm} \times 1\text{ mm}$ ($x \sim 0.2$), respectively. In order to ensure homogeneity of oxygen concentration the samples were appropriately annealed at 550°C as described in Ref. 16. This process is known to produce extremely homogeneous thin crystals of YBCO. The tetragonal c axis was normal to the large facet. The crystals were of high quality with a sample mosaic of $\sim 0.04^\circ$. Although the lateral dimensions of the crystals are large, the probed volumes were limited to a size of approximately $200\text{ }\mu\text{m} \times 200\text{ }\mu\text{m} \times 10\text{ }\mu\text{m}$ due to small beam size and absorption. The crystals were aligned so that the crystallographic directions $[1\ 1\ 0]$ and $[0\ 0\ 1]$ are both in the vertical scattering plane. This orientation allowed for reciprocal lattice scans in the $[H\ H\ L]$ zone to be carried out in the asymmetric Bragg reflection geometry. Scans in arbitrary directions through the accessible AF points, such as $(\frac{1}{2}, \frac{1}{2}, l)$, can of course be performed. The crystals were mounted inside a closed-cycle He refrigerator equipped with a high- T interface capable of varying the sample temperature from 10 K to 1000 K.

Figure 2 shows scans through the $(\frac{1}{2}, \frac{1}{2}, 9)$ point in reciprocal space where the AF Bragg peak is expected to appear. All the data were collected in the $\sigma\pi$ channel, which signifi-

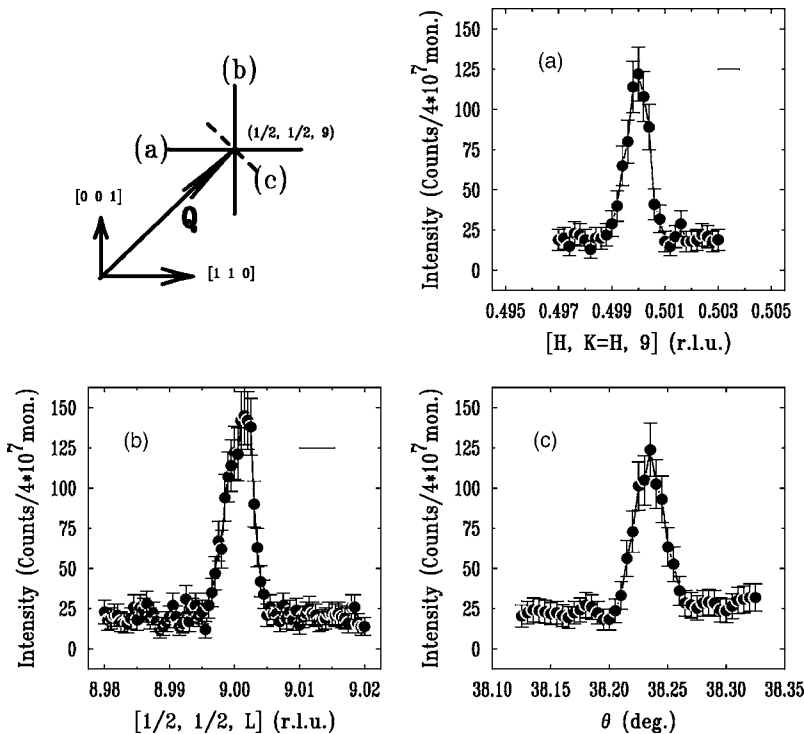


FIG. 2. Antiferromagnetic peak observed at $(\frac{1}{2}, \frac{1}{2}, 9)$ in the $\text{YBa}_2\text{Cu}_3\text{O}_{6.14}$ single crystal. At the top left corner, various scans are depicted by lines going through the $(\frac{1}{2}, \frac{1}{2}, 9)$ point with the plane of the paper defining the $[H\ H\ L]$ zone. (a) A scan along the $[1, 1, 0]$ direction; (b) A scan along $[0, 0, 1]$ which is perpendicular to the CuO_2 bilayers; (c) A transverse scan taken by rocking the sample. The horizontal lines indicate the instrumental resolution.

cantly suppresses Thomson scattering. A sharp Bragg peak characterized precisely by the AF wave vector, $\mathbf{q}_{\text{AF}}(\frac{1}{2}, \frac{1}{2}, 0)$, is clearly observed. The peak is resolution limited in both the [110] and [001] directions [Figs. 2(a) and 2(b)]. The half-widths-at-half-maximum are 0.0006 r.l.u. and 0.0025 r.l.u., respectively, indicating longer correlation lengths (~ 1000 Å) than those revealed by neutron-diffraction studies. The transverse scan [Fig. 2(c)] shows a width of $\sim 0.04^\circ$, which is comparable to the sample mosaic. Since the scattered photons in this channel have changed their state of polarization from σ to π and the scattering is observed at an x-ray energy far away from any resonances (i.e., x-ray absorption edges) we can conclude that the peak is magnetic in origin.

The observed count rate is 1–3 counts/s with a peak to background (average count rate away from the peak) ratio of 4–5, which should be compared with those in earlier neutron-diffraction studies.^{5–10} In those studies count rates varied between 0.3–7 counts/s with peak-to-background ratios in the range of 1–10. The count rate observed in the present study is consistent with the work by Hill and co-workers¹⁷ on $\text{PrBa}_2\text{Cu}_3\text{O}_7$ (PBCO), where magnetic scattering was resonantly enhanced twofold by tuning the x-ray energy to the Cu *K* edge. No direct observations of nonresonant magnetic scattering in their work were made.

In the absence of any orbital component to the magnetic moment, the nonresonant magnetic scattering amplitude can be written as follows:¹³

$$\begin{pmatrix} F^{\sigma\sigma} \\ F^{\sigma\pi} \end{pmatrix} \propto \begin{pmatrix} \mathbf{S}(\mathbf{Q}) \cdot (\hat{\mathbf{k}} \times \hat{\mathbf{k}}') \\ -\frac{Q^2}{2k^2} \mathbf{S}(\mathbf{Q}) \cdot \hat{\mathbf{k}}' \end{pmatrix}.$$

In this expression $\hat{\mathbf{k}}$ and $\hat{\mathbf{k}}'$ are the incident and scattered photon directions, $\mathbf{Q}=\hat{\mathbf{k}}-\hat{\mathbf{k}}'$ is the momentum transfer, and $\mathbf{S}(\mathbf{Q})$ is the Fourier transform (magnetic form factor) of the spin density, respectively. In the $\sigma\sigma$ channel, one measures the component of moments normal ($\parallel [1 \bar{1} 0]$) to the scattering plane, whereas, in the $\sigma\pi$ channel, moments lying within the scattering plane are measured. Note that, in this channel although the form factor decreases with increasing Q , the prefactor varies as Q^2 , making magnetic scattering slightly stronger compared to that in the $\sigma\sigma$ channel at the same momentum transfer. The magnetic peak strength in the $\sigma\sigma$ channel simply decreases with increasing Q according to $\mathbf{S}(\mathbf{Q})$. Furthermore, diffuse scattering (due to thermal and static disorder), which constitutes a significant background in the $\sigma\sigma$ channel and increases as Q^2 , makes the magnetic scattering in this channel more difficult to observe. Indeed, there was no detectable magnetic peak in the $\sigma\sigma$ channel consistent with the behavior of the cross section and diffuse scattering background. The lower Q region is not accessible in the scattering geometry employed to look for magnetic scattering in the $\sigma\sigma$ channel.

In their magnetic ground state, the copper moments antiferromagnetically order within the square CuO_2 planes with moments parallel to these planes. In YBCO, there are two such planes (bilayers) in a unit cell, and the moments in

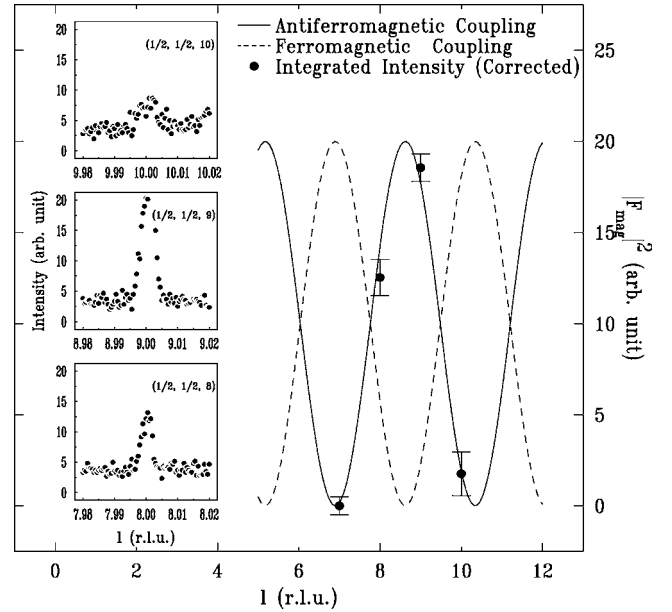


FIG. 3. Data showing how the structure factor is modulated due to the AF interlayer coupling of the copper spins. Insets show the scans through magnetic peaks. The scan through $(\frac{1}{2}, \frac{1}{2}, 7)$ did not show any peak above the background.

these neighboring planes are antiparallel to each other. Due to this anparallel spin alignment the integrated intensity ($|F_{\text{mag}}|^2$) of magnetic Bragg peaks varies as $\sin^2(\pi z l)$, where z is the interlayer separation in units of c , and l is the Miller index, along the [001] direction. Measured integrated intensities, corrected for geometric factors, of some magnetic peaks, illustrate this sinusoidal modulation convincingly (Fig. 3). For comparison the behavior of the intensities in the case of parallel (ferromagnetic) alignment of moments in these bilayers is also shown by the dashed line (Fig. 3), which manifestly disagrees with the data.

The temperature dependence of the integrated intensity of the strongest peak, $(\frac{1}{2}, \frac{1}{2}, 9)$, was studied in detail ($x \sim 0.14$), as shown in Fig. 4. Although there is some scatter in the data, the general trend is clear: a gradual decrease of intensity with increasing temperature. At 415 K no detectable intensity beyond the background was found. The entire temperature dependence can be described using a power law $I \propto (1 - T/T_N)^{2\beta} e^{-2W_{\text{Cu}}(T)}$ ($\beta = 0.19 \pm 0.04$), which gives a Néel

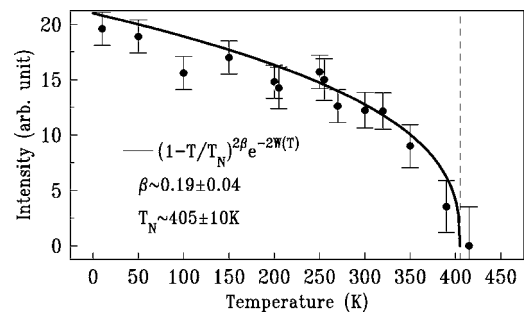


FIG. 4. Temperature dependence of the $(\frac{1}{2}, \frac{1}{2}, 9)$ magnetic peak. The solid line is the modeling of the data as discussed in the text. The vertical dashed line indicates the Néel temperature.

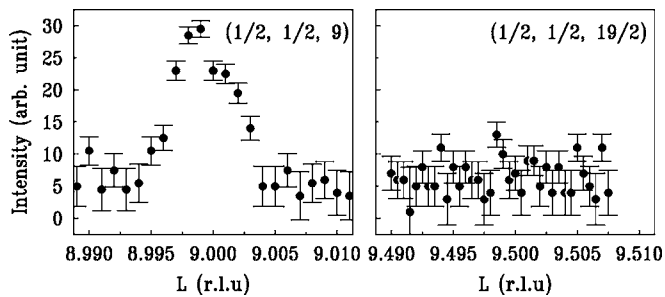


FIG. 5. Scans taken at a temperature of 10 K on a single-crystal YBCO sample with oxygen concentration of $x \sim 0.20$. Data were collected with the Ge analyzer removed.

temperature of 405 ± 10 K consistent with the expected transition temperature for this composition. Note that, in order to take into account the decrease in intensity due to thermal vibrations, we have included an exponential term with the Debye-Waller factor (DWF) of Cu (W_{Cu}) in the CuO_2 planes, in our modeling. The temperature dependent DWFs were estimated from Ref. 18.

As discussed above a low-temperature cell-doubling structure has been observed in a sample of YBCO with $x \sim 0.35$. Figure 5 shows scans through the $(\frac{1}{2}, \frac{1}{2}, 9)$ and $(\frac{1}{2}, \frac{1}{2}, \frac{19}{2})$ points taken on our sample with $x \sim 0.20$, at which the low- T phase is more likely to occur. While the \mathbf{q}_{AF} is observed, no signs of the cell-doubling structure are visible above the background. Our observation is consistent with the fact that a long-range-ordered low- T phase forms above an O concentration of $x \sim 0.2$, or the magnitude of the ordered moments in the CuO chains is significantly smaller. Since the

intensity of nonresonant magnetic scattering scales with the square of the ordered moments, we estimate an upper limit of this moment to be $\sim 0.2\mu_B$ noting that the ordered moment in the CuO_2 planes is $\sim 0.6\mu_B$.

To summarize, we report a “benchmark” study of direct nonresonant magnetic scattering of x rays from the AF phase of YBCO insulators. Magnetic Bragg peaks due to the AF state were measured entirely in the σ -to- π channel, and their intensities were consistent with the known AF structure and magnetic scattering cross section. According to our measurements, the AF state characterized by \mathbf{q}_{AF} in both the samples is very coherent ($\xi \sim 1000 \text{ \AA}$), consistent with the high quality of these crystals. Our work demonstrates how the non-resonant scattering technique can successfully study long-range-ordered spin- $\frac{1}{2}$ moments in oxides. Resonant x-ray scattering study performed on PBCO observed a twofold increase of the magnetic scattering intensity at the Cu K edge relative to the scattering intensity just below the edge.¹⁷ To date, no such studies have been performed on pure YBCO. Although the resonant enhancement is small a polarization-analyzer setup optimized for use exactly at the Cu K edge can improve the sensitivity to smaller moments and will be essential for future magnetic studies in cuprates.

We have benefited from discussions with D. E. Moncton and Y. S. Lee from MIT. Advanced Photon Source is supported by the U.S. DOE, Office of Basic Energy Sciences, Contract No. W-31-109-ENG-38. This work was supported in part by the Office of Basic Energy Sciences, U.S. Department of Energy Grant No. DE-FG02-03ER46084 (X.L. and S.K.S.).

*Email address: zahir@aps.anl.gov

- ¹D. Vaknin, S. K. Sinha, D. E. Moncton, D. C. Johnston, J. M. Newsam, C. R. Safinya, and H. E. King, Jr., *Phys. Rev. Lett.* **58**, 2802 (1987).
- ²S. Mitsuda, G. Shirane, S. K. Sinha, D. C. Johnston, M. S. Alvarez, D. Vaknin, and D. E. Moncton, *Phys. Rev. B* **36**, 822 (1987).
- ³S. K. Sinha, D. E. Moncton, D. C. Johnston, and D. Vaknin, *J. Appl. Phys.* **63**, 4015 (1988); S. K. Sinha, *Int. J. Mod. Phys. B* **1**, 799 (1987).
- ⁴N. Nishida *et al.*, *Jpn. J. Appl. Phys., Part 1* **26**, L1856 (1987); *J. Phys. Soc. Jpn.* **57**, 722 (1988).
- ⁵J. M. Tranquada, D. E. Cox, W. Kunmann, H. Moudden, G. Shirane, M. Suenaga, P. Zolliker, D. Vaknin, S. K. Sinha, M. S. Alvarez, A. J. Jacobson, and D. C. Johnston, *Phys. Rev. Lett.* **60**, 156 (1988).
- ⁶J. M. Tranquada, A. H. Moudden, A. I. Goldman, P. Zolliker, D. E. Cox, G. Shirane, S. K. Sinha, D. Vaknin, D. C. Johnston, M. S. Alvarez, A. J. Jacobson, J. T. Lewandowski, and J. M. Newsam, *Phys. Rev. B* **38**, 2477 (1988).
- ⁷D. Petitgrand and G. Collin, *Physica C* **153–155**, 192 (1988).
- ⁸P. Burllet, C. Vettier, M. J. G. M. Jurgens, J. Y. Henry, J. Rossat-Mignod, H. Noel, M. Potel, P. Gougeon, and J. C. Levet, *Physica C* **153–155**, 1115 (1988).
- ⁹W.-H. Li, J. W. Lynn, H. A. Mook, B. C. Sales, and Z. Fisk, *Phys. Rev. B* **37**, 9844 (1988).
- ¹⁰H. Kadowaki, M. Nishi, Y. Yamada, H. Takeya, H. Takei, S. M. Shapiro, and G. Shirane, *Phys. Rev. B* **37**, 7932 (1988).
- ¹¹J. W. Lynn, in *High Temperature Superconductivity*, edited by J. W. Lynn (Springer-Verlag, New York, 1990).
- ¹²J. P. Hannon, G. T. Trammell, M. Blume, and D. Gibbs, *Phys. Rev. Lett.* **61**, 1245 (1988).
- ¹³M. Blume and D. Gibbs, *Phys. Rev. B* **37**, 1779 (1988).
- ¹⁴M. D. Hamrick, M.A. thesis, Rice University (1991).
- ¹⁵D. Gibbs, D. E. Moncton, K. L. D’Amico, J. Bohr, and B. H. Grier, *Phys. Rev. Lett.* **55**, 234 (1985); D. E. Moncton, D. Gibbs, and J. Bohr, *Nucl. Instrum. Methods Phys. Res. A* **246**, 839 (1986).
- ¹⁶B. W. Veal, A. P. Paulikas, H. You, H. Shi, Y. Fang, and J. W. Downey, *Phys. Rev. B* **42**, 6305 (1990), and references therein.
- ¹⁷J. P. Hill, D. F. McMorrow, A. T. Boothroyd, A. Stunault, C. Vettier, L. E. Berman, M. v. Zimmermann, and Th. Wolf, *Phys. Rev. B* **61**, 1251 (2000).
- ¹⁸R. P. Sharma, F. J. Rotella, J. D. Jorgensen, and L. E. Rehn, *Physica C* **174**, 409 (1991); J. D. Jorgensen, B. W. Veal, A. P. Paulikas, L. J. Nowicki, G. W. Crabtree, H. Claus, and W. K. Kwok, *Phys. Rev. B* **41**, 1863 (1990).